The *Medicago truncatula* Lysine Motif-Receptor-Like Kinase Gene Family Includes *NFP* and New Nodule-Expressed Genes[1][W]

Jean-François Arrighi, Annick Barre, Besma Ben Amor[2], Anne Bersoult, Lidia Campos Soriano, Rossana Mirabella, Fernanda de Carvalho-Niebel, Etienne-Pascal Journet, Michèle Ghérardi, Thierry Huguet, René Geurts, Jean Dénarié, Pierre Rougé, and Clare Gough*

Laboratoire des Interactions Plantes-Microorganismes, Institut National de la Recherche Agronomique-Centre National de la Recherche Scientifique, Unité Mixte de Recherche 441/2594, 31326 Castanet-Tolosan, France (J.-F.A., B.B.A., A. Bersoult, F.C.-N., E.-P.J., M.G., T.H., J.D., C.G.); Surfaces Cellulaires et Signalisation chez les Végétaux, Centre National de la Recherche Scientifique-Université Paul Sabatier, Unité Mixte de Recherche 5546, Pôle de Biotechnologie Végétale, 31326 Castanet-Tolosan, France (A. Barre, P.R.); Laboratory of Molecular Biology, Wageningen University, 6703 HA Wageningen, The Netherlands (L.C.S., R.M., R.G.); and Laboratoire Biotechnologies et Amélioration des Plantes, Ecole Nationale Supérieure Agronomique Toulouse, 31326 Castanet-Tolosan, France (T.H.)

Rhizobial Nod factors are key symbiotic signals responsible for starting the nodulation process in host legume plants. Of the six *Medicago truncatula* genes controlling a Nod factor signaling pathway, *Nod Factor Perception* (*NFP*) was reported as a candidate Nod factor receptor gene. Here, we provide further evidence for this by showing that NFP is a lysine motif (LysM)-receptor-like kinase (RLK). *NFP* was shown both to be expressed in association with infection thread development and to be involved in the infection process. Consistent with deviations from conserved kinase domain sequences, NFP did not show autophosphorylation activity, suggesting that NFP needs to associate with an active kinase or has unusual functional characteristics different from classical kinases. Identification of nine new *M. truncatula* LysM-RLK genes revealed a larger family than in the nonlegumes Arabidopsis (*Arabidopsis thaliana*) or rice (*Oryza sativa*) of at least 17 members that can be divided into three subfamilies. Three LysM domains could be structurally predicted for all *M. truncatula* LysM-RLK proteins, whereas one subfamily, which includes NFP, was characterized by deviations from conserved kinase sequences. Most of the newly identified genes were found to be expressed in roots and nodules, suggesting this class of receptors may be more extensively involved in nodulation than was previously known.

Whereas many interactions between higher plants and microorganisms are beneficial for one of the partners, few such interactions benefit both partners. The association between bacteria called rhizobia and legume plants is a good example of a mutually beneficial interaction. Rhizobia induce nitrogen-fixing nodules on legume plants, thus allowing plant growth to be independent of an added nitrogen source and, in return, the plant provides rhizobia with a carbon source derived from photosynthesis. Rhizobial Nod factors are crucial symbiotic signals responsible for inducing nodule organogenesis and host-specific, controlled infection (Dénarié et al., 1996). All Nod factors are lipochitooligosaccharidic molecules, consisting of an oligomeric backbone of β-1,4-linked GlcNAc residues that carries an *N*-acyl chain on the nonreducing end residue. The backbone has four to five residues and diverse substitutions on the nonreducing- and reducing-end GlcNAc residues, which are major molecular determinants of host specificity. At nano- to picomolar concentrations, Nod factors elicit diverse plant symbiotic responses in host roots (Riely et al., 2004).

Candidate Nod factor receptor genes have been cloned in model legumes and pea (*Pisum sativum*). These genes, called *LYK3* in *Medicago truncatula* (Limpens et al., 2003), *NFR1* and *NFR5* in *Lotus japonicus* (Madsen et al., 2003; Radutoiu et al., 2003), and *SYM10* in pea (Madsen et al., 2003), are predicted to encode lysine motif (LysM)-receptor-like kinases (RLKs), members of the superfamily of plant RLKs. The LysM domains of these proteins, being predicted to be both extracellular and sites of interaction with GlcNAc-containing

[1] This work was supported by the French Ministère de l'Education Nationale, de l'Enseignement Supérieur et de la Recherche (doctoral grants to J.F.A. and A. Bersoult), by the French government in the frame of Tunisian cooperation (doctoral grant to B.B.A.), and by the Agence Nationale de la Recherche (project NT05–4–42720).

[2] Present address: Institut des Sciences du Végétal, Centre National de la Recherche Scientifique, 91198 Gif sur Yvette, France.

* Corresponding author; e-mail gough@toulouse.inra.fr; fax 33–561285061.

The author responsible for distribution of materials integral to the findings presented in this article in accordance with the policy described in the Instructions for Authors (www.plantphysiol.org) is: Clare Gough (gough@toulouse.inra.fr).

[W] The online version of this article contains Web-only data.
www.plantphysiol.org/cgi/doi/10.1104/pp.106.084657

compounds (Steen et al., 2003, 2005), are hypothesized to be the regions of these putative receptors that interact with Nod factors. In *L. japonicus*, *nfr1* and *nfr5* mutants have the same phenotype, suggesting that NFR1 and NFR5 constitute a heterodimeric receptor (Madsen et al., 2003). Following ligand recognition, it is supposed that downstream signal transduction would involve the intracellular kinase domains.

In *Medicago* spp., pea, and vetch (*Vicia sativa*), which form indeterminate nodules, early steps of infection are particularly stringent in terms of Nod factor structure, whereas some other Nod factor-dependent responses are less stringent, suggesting different mechanisms of Nod factor perception (Ardourel et al., 1994; Geurts et al., 1997; Walker and Downie, 2000; Catoira et al., 2001). The *M. truncatula LYK3* gene, the probable ortholog of *L. japonicus NFR1*, has been proposed to encode an entry receptor controlling Nod factor recognition for infection thread initiation and growth (Limpens et al., 2003). This suggests that, in *M. truncatula*, one or more other Nod factor receptors would control earlier steps of Nod factor recognition.

Analysis of the *M. truncatula* mutant C31 showed that the *Nod Factor Perception* (*NFP*) gene plays an essential role in Nod factor perception at early steps of the symbiotic interaction (Ben Amor et al., 2003) and, as such, is another candidate Nod factor receptor gene. In *M. truncatula*, *NFP* is predicted to control a Nod factor signaling pathway in which the genes *DMI1*, *DMI2*, *DMI3*, *NSP1*, and *NSP2* act downstream of *NFP* to control symbiotic responses and nodulation (Catoira et al., 2000; Wais et al., 2000; Ben Amor et al., 2003; Oldroyd and Long, 2003). The transcriptional changes observed using macro- and microarrays in wild-type *M. truncatula* plants following rhizobial inoculation are not observed in *nfp*, *dmi*, or *nsp* mutants (El Yahyaoui et al., 2004; Mitra et al., 2004b), supporting the importance of this pathway. Important insights into the Nod factor signaling pathway in *M. truncatula* have come from the cloning of *DMI1*, *DMI2*, *DMI3*, *NSP1*, and *NSP2* (Endre et al., 2002; Ané et al., 2004; Lévy et al., 2004; Mitra et al., 2004a; Kalo et al., 2005; Smit et al., 2005). Recent results suggest coordinated expression of these genes, as well as *LYK3*, in the infection zone of nodule apices (Bersoult et al., 2005; Limpens et al., 2005), suggesting that Nod factor perception and signaling are required throughout nodulation.

In this study, our initial aim was to better define the role and functioning of the *NFP* gene in the establishment of the Rhizobium-legume interaction. This led us to show that *NFP* codes for a LysM-RLK that did not show autophosphorylation activity and that is expressed throughout the nodulation process. We then exploited the genomic resources of *M. truncatula* to identify other LysM-RLK genes. This revealed a relatively large gene family, including several new genes that are expressed in roots and nodules, suggesting that LysM-RLKs may be more extensively involved in nodulation than was previously known.

RESULTS

The *NFP* Gene of *M. truncatula* Encodes a LysM-RLK

We had previously suggested that *NFP* and pea *SYM10* could be orthologous genes (Ben Amor et al., 2003). Based on this, the sequence of *SYM10* (Madsen et al., 2003) was used to search sequence databases of *M. truncatula*. A good candidate gene for *NFP* was identified by an expressed sequence tag (EST) and a bacterial artificial chromosome (BAC) clone. Using the mapping population generated for *NFP* (Ben Amor et al., 2003), the candidate gene was inseparable from the *NFP* locus (data not shown). The candidate gene was sequenced in two *nfp* mutants; C31 (*nfp-1*; Ben Amor et al., 2003) and T1-6 (*nfp-2*), a new *nfp* mutant isolated by screening mutagenized *pMtENOD11-β*-glucuronidase (GUS) plants for the absence of Nod factor induction of the GUS fusion. *nfp-2*, just like *nfp-1*, is Nod^- in response to *Sinorhizobium meliloti*, with no root hair curling or infection thread formation and no Nod factor-induced root hair deformation (data not shown). In each case, a mutation was found within the first part of the coding region, giving rise to a stop codon for *nfp-1* and a Ser residue replaced by a Phe for *nfp-2* (Fig. 1). Roots of the *nfp-1* mutant were transformed using *Agrobacterium rhizogenes*, with the candidate gene including 1.1 kb of the promoter region. Following inoculation with *S. meliloti*, nodules were formed on 57 of 85 plants (six nodules/plant on average), whereas *nfp-1* transformed with the vector alone did not nodulate (no nodules on 76 plants). This functional complementation provides the final proof that the candidate gene corresponds to *NFP*.

The *NFP* gene has no introns and is predicted to encode a protein of 595 amino acids, consisting of an N-terminal signal peptide, followed by a LysM-RLK domain structure made up of three predicted LysM domains in the putative extracellular part of the protein, a potential transmembrane helix, and a Ser-Thr kinase domain in the C-terminal part. This predicted protein sequence shows 86% and 72% overall identity with SYM10 and NFR5, respectively (Fig. 1). As previously reported for SYM10 and NFR5, 27 amino acids corresponding to a normally well-conserved part of the kinase domain, the so-called activation loop, are missing in NFP (Fig. 1). All three proteins also lack the so-called P-loop or phosphate anchor (GXGXF/YG) as well as a conserved DFG motif next to the missing activation loops, regions normally highly conserved in protein kinases (Fig. 1).

NFP Is Expressed in Association with Primordium Formation and with Infection throughout the Nodulation Process

Given that *nfp* mutants were selected for their null phenotypes, we cannot exclude that *NFP* is implicated not only for early Nod factor signaling, but also at later stages of the symbiotic interaction. To address this question, we studied the spatiotemporal expression

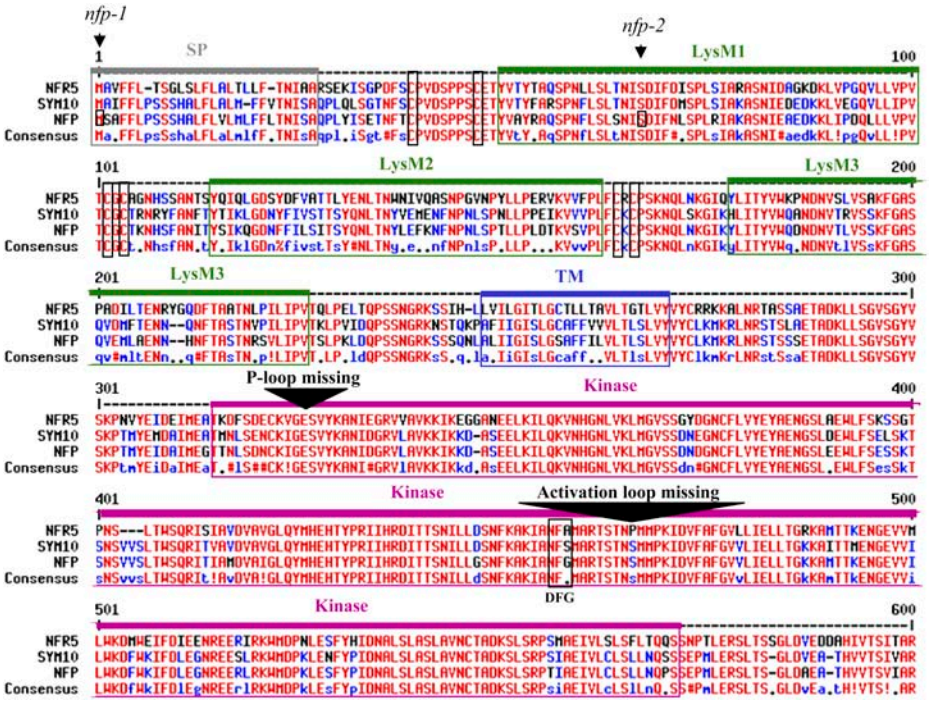

Figure 1. Amino acid alignment of NFP (*M. truncatula*), SYM10 (pea), and NFR5 (*L. japonicus*), showing conserved domain structure and conserved Cys residues in the predicted extracellular parts (boxed). Sites where the P-loops, activation loops, and the DFG motifs are missing are indicated. In NFP, positions of mutations found in *nfp-1* (residue no. 1) and *nfp-2* (residue no. 67) are boxed and indicated by arrowheads. SP, Signal peptide; LysM1, LysM2, and LysM3, three LysM domains; TM, transmembrane segment.

pattern of the *NFP* gene using promoter-GUS fusions and roots of *M. truncatula* transformed by *A. rhizogenes*. The 1.5-kb fragment in these constructions included the same 1.1-kb promoter region used for the functional complementation described above.

Noninoculated roots showed strong GUS activity in root hair cells of lateral roots (Fig. 2A). Older regions of roots showed low or no GUS activity. One day after inoculation with *S. meliloti*, GUS activity was restricted to discrete areas of the epidermis (Fig. 2B). At 2 d, GUS activity was associated with the inner cortex, forming broad stained regions where cell divisions corresponding to the formation of nodule primordia could be observed. GUS activity subsequently extended to the middle cortex of regions where root hairs could be seen to be undergoing root hair curling, the first step of infection (Fig. 2C). At 3 d, GUS activity was detected in outer cortical cells directly underlying infected root hairs and through which infection threads were subsequently seen to pass (Fig. 2, D and E). At 5 d, GUS staining was very intense in the central nodule tissue of young, emerging nodules, which mainly consists of cells undergoing infection by the highly ramified infection thread network (Fig. 2F). In mature nodules, GUS activity was restricted to the infection zone, showing strongest staining in cell layers directly adjacent to the meristem (Fig. 2, G and H). Much lower expression was visible in interzone II/III and no expression was detected in the nitrogen-fixing zone (Fig. 2, G and H). This is clearly illustrated in nodules in which bacteria were not stained (Fig. 2I).

For mature nodules, we verified by in situ hybridization that this localization of GUS activity accurately reflected *NFP* expression. *NFP* transcripts were detected in a relatively broad area of mature nodule apices, with the highest level corresponding to the most distal part of the infection zone, as found with the Pro_{NFP}-*GUS* fusion (Fig. 2, J and K). Consistent with 1.1 kb of this 1.5-kb promoter fragment being sufficient for functional complementation of the *nfp* mutation, this indicates that the major cis-acting elements required for cell-specific expression of *NFP* are present in the 1.5-kb *NFP* promoter fragment. Furthermore, this shows that *NFP* expression is associated with the infection process.

Knockdown of *NFP* Suggests a Role for *NFP* during Infection Thread Formation

We investigated the role of *NFP* in the infection process using RNA interference (RNAi) constructs and *A. rhizogenes*-mediated root transformation of *M. truncatula*. We expected to produce roots with a range of knockdown levels, some of which could show weak phenotypes for infection and nodulation. Two independent *NFP* interference constructs were analyzed, *NFPi1* and *NFPi2*, which correspond to the LysM and kinase domains, respectively.

The majority of *NFP* knockdown roots were Nod^- following inoculation with *S. meliloti*: 79% of *NFPi1* and 90% of *NFPi2* roots (i.e. a total of 21/24 Nod^- roots). The rare nodules formed showed a wild-type structure when sectioned (data not shown). For control roots, 100% were efficiently nodulated with 11 nodules per root on average. Because the nodulation phenotype for the *NFP* knockdown roots is, in most cases, similar to

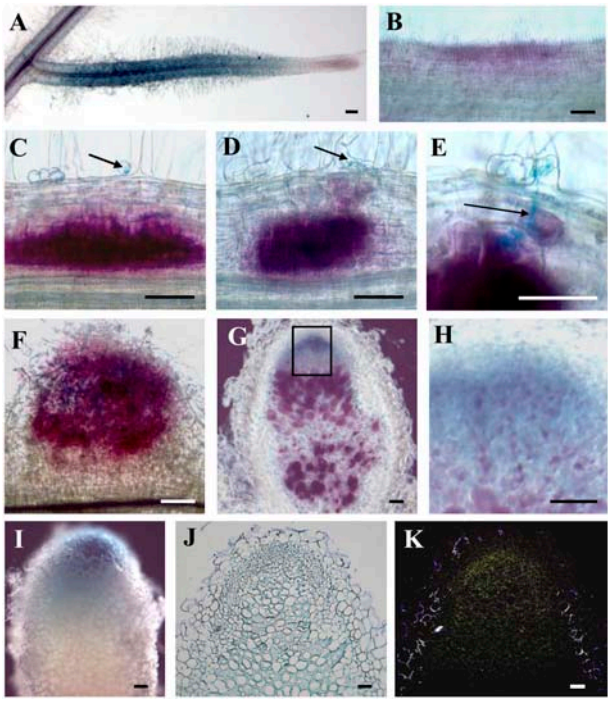

Figure 2. Localization of *NFP* gene expression throughout nodulation in *M. truncatula*. A to H, Expression of a Pro_{NFP}-*GUS* fusion in transgenic roots, inoculated or not with *S. meliloti*. A, Whole, non-inoculated lateral root showing constitutive GUS activity (blue) in root hairs. B to F, Root segments showing GUS activity (magenta) in the epidermis 1 d postinoculation (dpi; B), in the inner and middle cortex where cell divisions are occurring under a curled root hair (arrow) at 2 dpi (C), in the inner and middle cortex 2 dpi, and in outer cortical cells (D), in outer cortical cells through which an infection thread (arrow) is passing (E), and in an emerging nodule 5 dpi (F). G and H, Longitudinal section of an 18-d-old nodule showing GUS activity (blue) in the apical region and bacteria (magenta) in infection threads and the nitrogen-fixing zone. H, Close-up of the box in G. I, GUS activity (blue) in an 18-d-old whole nodule, with bacteria not stained. J and K, In situ hybridization of *NFP* gene expression on a sectioned 14-d-old nodule using a ^{35}S-UTP labeled antisense *NFP* probe. Bright-field image of nodule section with silver grains visible in black (J); epipolarization image of I (K). Arrows indicate points of infection in root hair curls (C and D) and an infection thread (E). Bars = 100 μm.

the knockout phenotype, it can be assumed that there is efficient silencing in these roots, whereas incomplete silencing has occurred in the three Nod$^+$ roots.

When rhizobia were visualized, 37 $\pm$ 12 infection threads were seen per control root. These were always tubular structures (Fig. 3A), but about 10% stopped abruptly in root hair cells. Infection structures were not seen on nonnodulated roots of *NFPi* plants, but were observed on nodulated *NFPi1* roots in regions adjacent to nodules: 12 and six infection threads for the two *NFPi1* roots exhibiting 10 and nine nodules, respectively. These infection threads nearly always aborted in root hairs and often had aberrant morphology, consisting of large sac-like structures (Fig. 3, B and C). This type of infection thread was never seen on control roots.

Two lines of evidence support the assumption that silencing in *NFP* knockdown roots was specific for *NFP* transcripts. First, within the two regions used for *NFP* RNAi, there is no 21-bp region showing 100% identity between *NFP* and any known member of the *M. truncatula* LysM-RLK gene family described below. Second, RNAi performed on LYR1, the gene most homologous to *NFP* (see below), did not result in a Nod$^-$ phenotype and infection threads were normal (data not shown).

Taken together, these results suggest a role for NFP in infection thread formation in agreement with *NFP* gene expression data.

The NFP Kinase Domain Does Not Show Autophosphorylation Activity

In the NFP kinase domain, deviations were observed in the activation loop and in the P-loop, as well as in the DFG motif (Fig. 1), which are normally highly conserved in Ser-Thr kinases, and play important roles in positioning ATP and the Ser-Thr substrate. The NFP kinase domain might therefore be inactive. In contrast, the LYK3 kinase domain is fully conserved and predicted to be fully active.

To gain further insight into these possibilities, we studied the autophosphorylation abilities of NFP and LYK3. The RLK BAK1 was used as a positive control (Li et al., 2002). N-terminal glutathione *S*-transferase (GST)-tagged intracellular domains of these three proteins (called GST-NFP, GST-LYK3, and GST-BAK1) were expressed in *Escherichia coli* and purified on glutathione Sepharose columns. The purified proteins were incubated with a kinase buffer containing [γ-^{32}] P-labeled ATP and separated by SDS-PAGE followed by Coomassie Blue staining (Fig. 4A). Phosphorylated proteins were visualized by phosphor imaging (Fig. 4B). We detected phosphorylation of the GST-LYK3 and GST-BAK1 proteins, but not the GST-NFP protein, indicating that the intracellular domain of LYK3, but

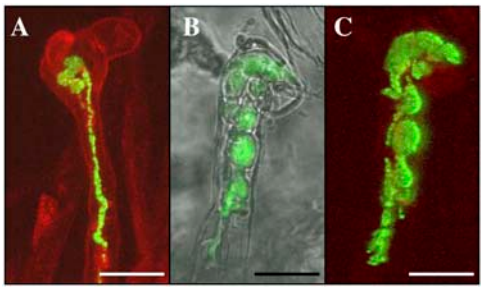

Figure 3. Analysis of the role of NFP in controlling infection thread formation. Roots of wild-type *M. truncatula* plants were transformed with either the vector alone (A) or an RNAi construct for *NFP* (B and C). Confocal images of root hairs in which GFP-expressing *S. meliloti* are seen in infection threads, which are tubular for the control and sac-like in *NFPi* root hairs. Root hairs in A and C were counterstained by propidium iodide (0.2 μg/mL). Bars = 10 μm.

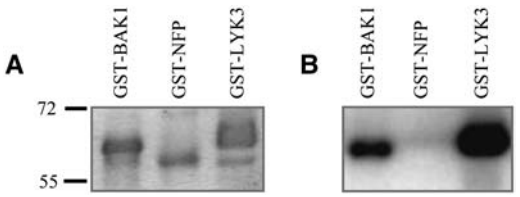

Figure 4. Autophosphorylation tests on the intracellular kinase domains of NFP and LYK3. Purified GST-tagged intracellular domains of NFP, LYK3, and BAK1 (GST-NFP, GST-LYK3, and GST-BAK1) were assayed for autophosphorylation activity using [γ-^{32}P]ATP. Reactions were subjected to SDS-PAGE and proteins visualized with Coomassie Blue (A). Phosphorylated proteins were visualized by phosphor imaging (B). Molecular mass markers of 55 and 72 kD are shown.

not of NFP, shows autophosphorylation activity in the conditions tested.

The *M. truncatula* Genome Contains a LysM-RLK Family of at Least 17 Genes

We were intrigued that, although NFP and LYK3 are both candidate Nod factor receptors, they differ in their kinase domains and in the number of predicted LysM domains (three and two, respectively). To determine whether such variations are specific to these two proteins, we characterized the *M. truncatula* LysM-RLK family. We first performed in silico searches in *M. truncatula* EST and genomic databases and, given the very large number of kinase-encoding genes in plant genomes (more than 400 RLKs alone in Arabidopsis [*Arabidopsis thaliana*]), we used LysM domains. Then, because LysM domains are not always associated with kinase domains, we made a preselection among ESTs and only sequenced those most similar to LysM domains of Arabidopsis LysM-kinase proteins. In addition to *NFP* and the previously identified *LYK* gene cluster (*LYK1–7*; Limpens et al., 2003), nine new potential LysM-RLK genes were identified and, as explained below, named *LYR1* to *6* and *LYK8* to *10*. All except *LYR1* were represented as ESTs and six genes (*LYR1*, *3–6*, and *LYK10*) as genomic sequences with one (*LYR1*, *3*, and *4*), two (*LYR5* and *6*), and 10 (*LYK10*) exons, and the LysM-encoding part is always devoid of introns.

All nine corresponding proteins are predicted to have an N-terminal signal peptide, one or more LysM domains in the predicted extracellular regions (Pfam predictions), a transmembrane-spanning segment of 22 to 23 predominantly hydrophobic residues, and a Ser-Thr kinase domain in the predicted cytoplasmic part of the protein. Alignments with NFP and LYK1 to 7 (except LYK5 because *LYK5* is probably a pseudogene; Limpens et al., 2003) showed that certain residues are highly conserved in the extracellular parts, including two repeats of Cys-X-Cys, which, for NFP, are located first between LysM1 and LysM2 and second between LysM2 and LysM3 (Supplemental Fig. 1).

Sequence conservation is strongest in the putative intracellular kinase domains, but close inspection revealed that, in addition to LYK3, LYR5 and 6 and LYK1, 2, 4, and 6 to 9 have fully conserved kinase domains, whereas those of LYK10, and LYR1 to 4 are like NFP in having deviations in normally conserved residues (Supplemental Fig. 1). In LYK10, the conserved Thr-Ser residue in the activation loop is replaced by a Glu residue. In LYR1 to 4 kinase domains, the P-loop is missing and the DFG motif is substituted. LYR1 also lacks the activation loop. In addition, the catalytic Asp residue is replaced by Asn in LYR1 and 4, and the conserved Thr-Ser residue in the activation loops of LYR3 and 4 is replaced by Asp. Based on this, as well as sequence length, overall homology and structural predictions of the extracellular parts of these proteins (see below), four major groups of *M. truncatula* LysM-RLKs were distinguished and are represented schematically in Figure 5.

These results show that the LysM-RLK gene family in *M. truncatula* consists of at least 17 genes, more than in either of the nonlegume plants Arabidopsis (five genes) or rice (*Oryza sativa*; six genes), and with six showing variation in conserved kinase residues.

The *M. truncatula* LysM-RLK Family Is Divided into Three Subfamilies

Based on kinase domain phylogeny, Arabidopsis and rice LysM-RLK proteins form two clades, LysM-I and LysM-II (Shiu et al., 2004). These were distinguished

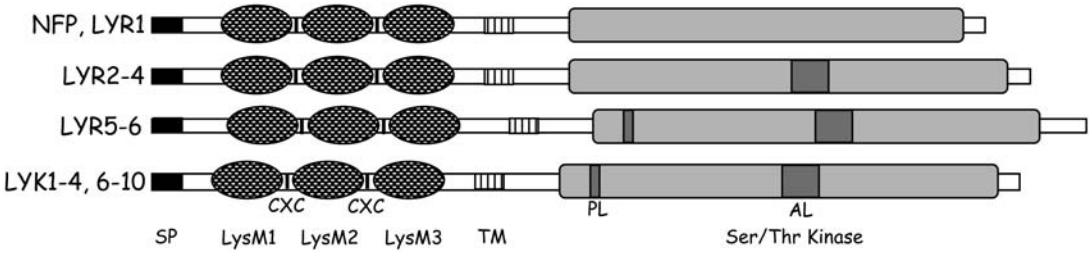

Figure 5. Schematic representation of the domain structure of 16 *M. truncatula* LysM-RLKs, based on the amino acid alignment presented in Supplemental Figure 1 and protein domain predictions explained in the text. SP, Signal peptide; LysM1, LysM2, and LysM3, three LysM domains; CXC, Cys-X-Cys motif; TM, transmembrane segment; PL, P-loop; AL, activation loop; Ser-Thr kinase, predicted intracellular kinase domain.

when we explored the phylogenetic relationships among kinase domains of the *M. truncatula* LysM-RLK family, together with those of the five similar proteins of Arabidopsis and six of rice and NFR1 and NFR5 of *L. japonicus*, with LYK3 and NFP belonging to the LysM-I and the LysM-II subfamilies, respectively (Fig. 6). A third group, LysM-III, consisted only of the *M. truncatula LYR5/6* genes (Fig. 6).

Comparison of intron/exon organization (known for all Arabidopsis and rice genes, *NFR1* and *NFR5*, and 13 *M. truncatula* genes) with clades indicated that LysM-I clade genes have 10 to 12 exons, whereas LysM-II and LysM-III genes have one and two exons, respectively. The nomenclature adopted for the new *M. truncatula* genes is based on these important and clear differences in gene structure. Thus, the previously adopted *LYK* (LysM domain-containing RLK) has been used for genes having 10 to 12 exons, and other new genes are called *LYR* (for LYK-related). Consistent with several deviations from the consensus kinase sequence in NFP and LYR1 to 4, these proteins cluster together in the LysM-II clade, where NFP and LYR1 (both lacking an activation loop) form a distinct subgroup. In both of the other clades (LysM-I and LysM-III), all kinases have classical conserved sequences, except LYK10.

The same correlation was found between clade and conservation of key kinase residues for Arabidopsis

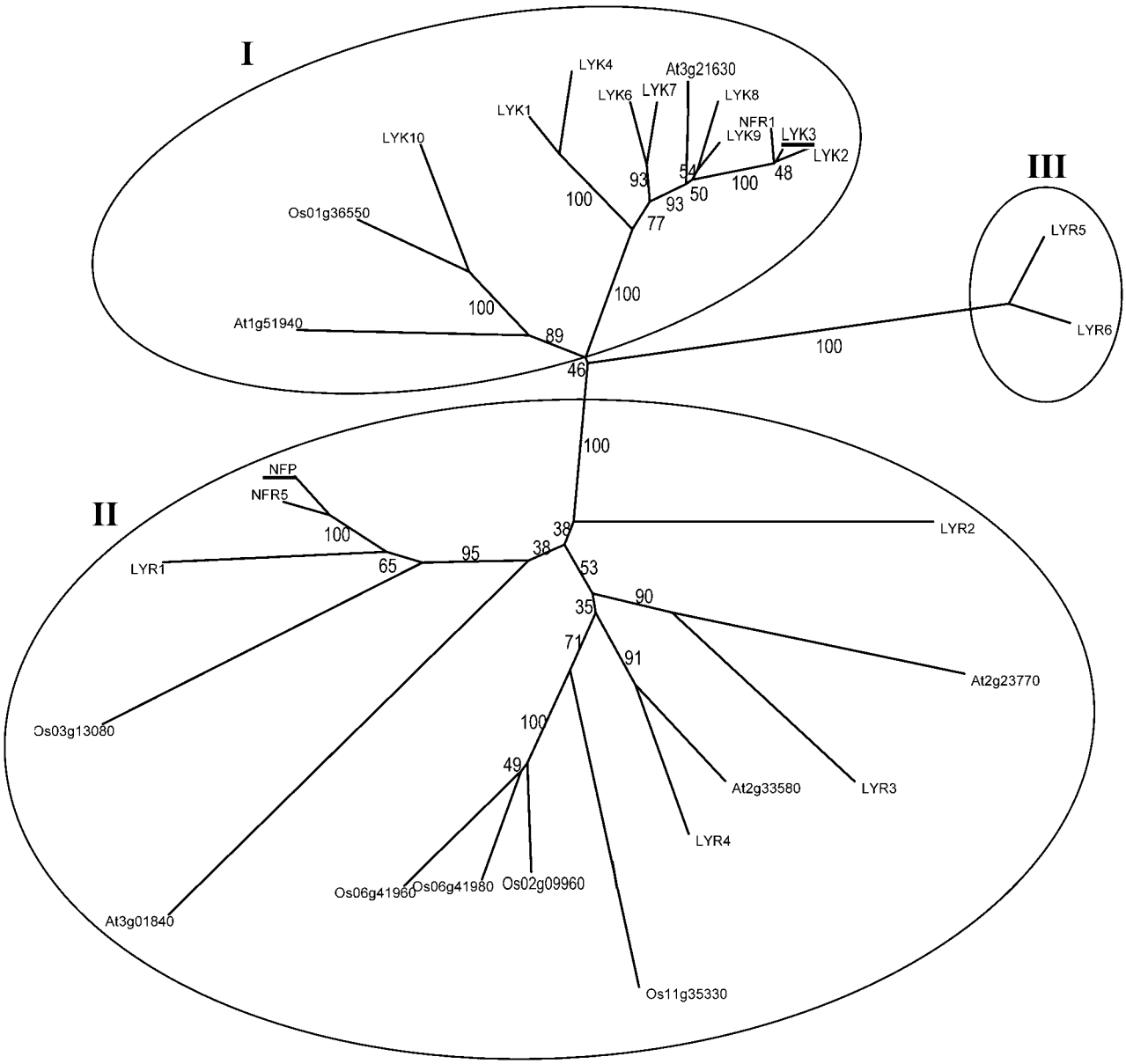

Figure 6. Phylogenetic tree of kinase domains of LysM-RLK proteins of *M. truncatula* (16), rice (six), Arabidopsis (five), and NFR1 and NFR5 of *L. japonicus*, showing bootstrap values. NFP and LYK3 are underlined and the three groups are labeled I, II, and III.

and rice LysM-RLK kinase domains, with Os03g13080 in LysM-II even missing the activation loop exactly as for NFP and LYR1. The only exceptions involved At1g51940 and Os01g36550 in LysM-I, which, like LYK10, lack a normally conserved Ser-Thr residue in their activation loops. This indicates that all LysM-II clade proteins either have substantially reduced kinase activity or unusual functional characteristics different from classical kinases, whereas the majority of LysM-I and all LysM-III proteins have normal kinase activity.

Finally, according to structural similarity between Ser-Thr kinases and the human Tyr kinase (PDB code IFIN; Jeffrey et al., 1995), in silico models were built for LYK3 and NFP kinase domains as representatives of LysM-I and LysM-II kinases, respectively (Supplemental Fig. 2). Canonical three-dimensional (3-D) structures were predicted for both and the only significant difference concerned the region of the activation loop, which, of course, is missing in the structure of NFP (Supplemental Fig. 2).

Three LysM Domains Are Structurally Predicted for Each *M. truncatula* LysM-RLK

We analyzed extracellular domains of *M. truncatula* LysM-RLK proteins by in silico modeling to determine how many LysM domains are predicted within each protein and whether each LysM domain is likely to be equivalent in terms of potential ligand binding.

Based on positions of the Cys-X-Cys motifs, three potential LysM domains were identified for each protein and used to make 3-D structural models. Hydrophobic cluster analysis (HCA) plots were generated and compared to the HCA plot of the murein hydrolase from *E. coli*, for which there is an NMR-solved LysM domain structure (Bateman and Bycroft, 2000; Supplemental Data 1). This *E. coli* LysM domain has a globular structure with a shallow groove on the surface, thought to be the site for peptidoglycan binding. The structural backbone of this domain is formed of two strands of a β-sheet (β1, β2) flanking two short α-helices (α1, α2). Despite the moderate percentages of identity (approximately 25%) and similarity (approximately 67%) between the *E. coli* and *M. truncatula* LysM domains, these structures were easily delineated on the HCA plots of all the *M. truncatula* sequences (illustrated for NFP in Fig. 7), indicating pronounced 3-D structural conservation and the presence of three LysM domains in each of the 16 proteins analyzed (NFP, LYR1–6, LYK1–4, and LYK6–10).

For NFP and LYK3, LysM domains differ from their *E. coli* counterparts in some insertions or deletions occurring in loop regions and by their charges. LysM1 domains are essentially electropositively charged (net charge from 2–4) or neutral, but LysM2 (net charge from -2 to -4) and LysM3 (net charge from -1 to -5) are predominantly electronegative (illustrated for NFP in Fig. 7). The electropositively (Arg, Lys) or electronegatively (Asp, Glu) charged residues mainly occur in loop regions and there is a strongly electropositive cavity in LysM2 of NFP, but not in LysM2 of LYK3 (Fig. 7; data not shown).

Close inspection of the amino acid alignment in Supplemental Figure 1 indicated a certain level of conservation among equivalent LysM domains of different proteins. To study this further, separate alignments were made of domains in the same position of each protein to take into account structurally homologous amino acids. Supplemental Figure 3 shows that LysM1, LysM2, and LysM3 of one protein have several structurally homologous amino acids in common with the same domain of other LysM-RLK proteins, but not with other domains of the same protein. This suggests that, in addition to the overall conserved 3-D structures, and the differences in charge between different domains in NFP and LYK3, certain structural features are unique to each domain.

Seven New LysM-RLK Genes Are Expressed in Roots and Nodules

We performed quantitative reverse transcription (RT)-PCR for the nine new *M. truncatula* genes, as well as *NFP*, using RNA extracted from symbiotic (roots and nodules) and nonsymbiotic (leaves and stems) plant tissues (Table I). As a result, four classes of expression pattern could be distinguished. In the first class, *LYR2* and *LYK10* were expressed specifically in roots and nodules. In the second class, *NFP*, *LYR3*, and *LYR6* were expressed in roots and nodules and at a much lower level in leaves or stems. In the third class, *LYR1* and *LYK8* are expressed mostly or only in roots. Finally, *LYR4*, *LYR5*, and *LYK9* were expressed in all tested tissues, with the highest levels in leaves. Table I also shows the relative expression levels in roots of new genes compared to *NFP*, indicating that the majority are more highly expressed than *NFP*.

These results indicate that *NFP*, like other previously characterized symbiotic LysM-RLK genes (Limpens et al., 2003; Madsen et al., 2003; Radutoiu et al., 2003), is preferentially expressed in nonaerial parts of the plant. Furthermore, six new genes (*LYR1*, *LYR2*, *LYR3*, *LYR6*, *LYK8*, and *LYK10*) were expressed predominantly in roots and nodules.

LysM-RLKs Have Expanded in the *M. truncatula* Genome by Gene Duplication and Segmental Genome Duplication

As for RLK gene expansion in Arabidopsis (Shiu and Bleecker, 2003), both tandem duplication and segmental genome duplication appear to have occurred for the *M. truncatula* LysM-RLK family. Thus, *LYK3* is in a cluster of seven *LYK* genes (Limpens et al., 2003), which shows microsynteny to a second region of chromosome 5 (Gualtieri and Bisseling, 2002). For new genes, we identified two tandem repeats: *LYR3*/*NFP* and *LYR5*/*LYR6*. Also, highly homologous pectate lyase genes were found adjacent to both *LYR3*/*NFP*

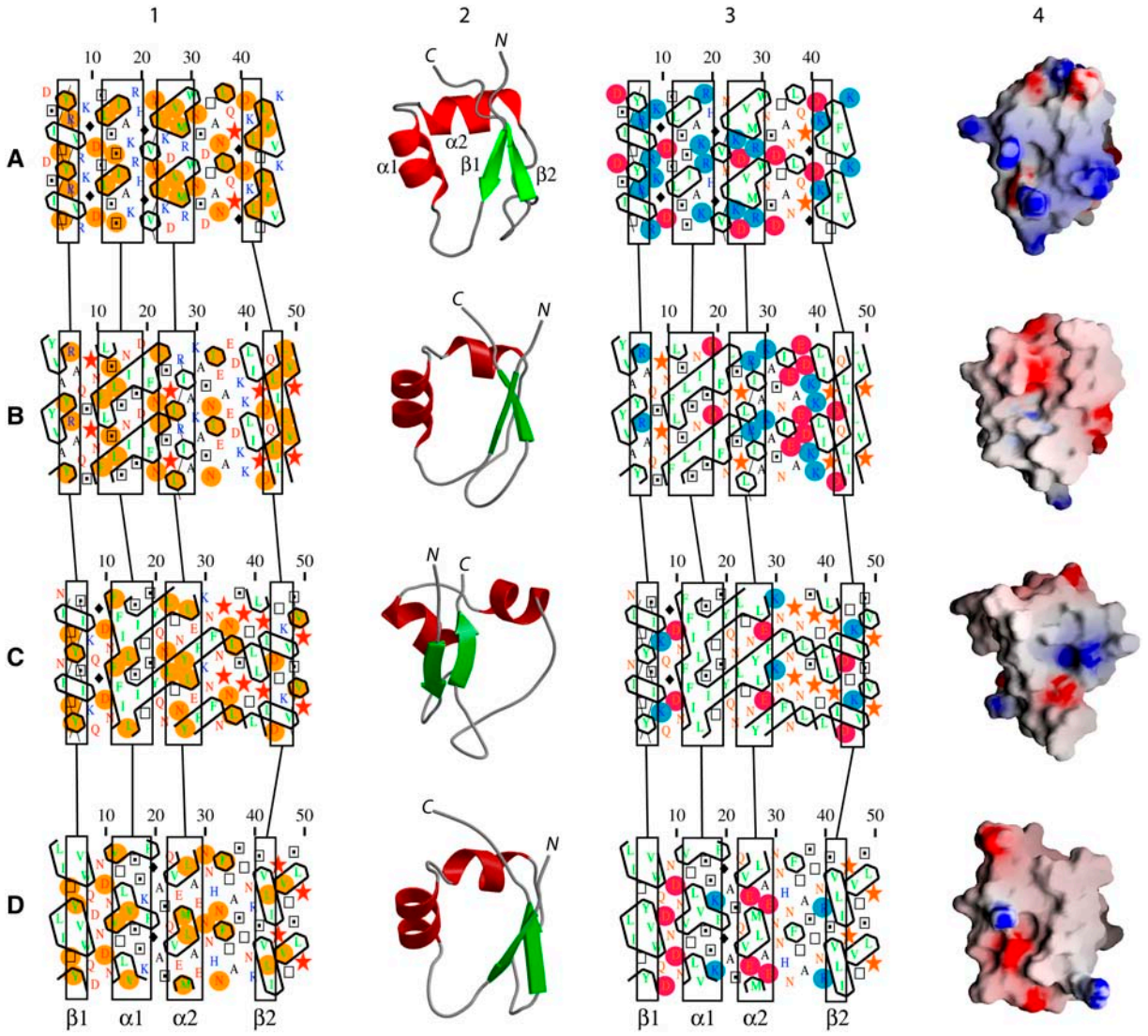

Figure 7. Structural predictions for LysM domains of NFP. 1 and 3, HCA plots showing homologous hydrophobic residues (circled orange) and secondary structural features (boxed; 1) and electropositively (circled blue) and electronegatively (circled red) charged residues (3). 2, Ribbon diagrams showing the N- and C-terminal ends of the LysM domain polypeptides. 4, 3-D models with electrostatic potentials displayed on the molecular surface of LysM domains at −5 kT and +5 kT levels; red (electronegative), blue (electropositive), and white (neutral). A, LysM domain of *E. coli* murein hydrolase. B to D, Structural predictions for NFP LysM domains built from the atomic coordinates of this *E. coli* LysM domain: LysM1 (B); LysM2 (C); LysM3 (D). Note the strongly electropositive cavity in LysM2 of NFP (4C).

and *LYR1* (but not to *LYR5*/*LYR6*), and remnants of LysM genes were found adjacent to *LYR1*, suggesting chromosomal segmental duplication followed by sequence changes for the *LYR3*/*NFP* and *LYR1* regions.

To further characterize genomic organization of LysM-RLKs, we used the *M. truncatula* genetic map (Thoquet et al., 2002) and positioned new LysM-RLK genes on six of the eight chromosomes of *M. truncatula* (Fig. 8). The highest density of LysM-RLK genes is on chromosome 5 (11 of 17 genes), where *NFP* and the *LYK1* to *7* gene cluster map (Ben Amor et al., 2003; Limpens et al., 2003). On this chromosome, although *LYR4* and the *LYK1* to *7* gene cluster genetically colocalize, analysis of BAC contigs showed that they could be physically separated.

This analysis indicates that both tandem duplication and segmental genome duplication events are responsible for the large *M. truncatula* LysM-RLK gene family. Furthermore, 11 of the 17 identified *M. truncatula* LysM-RLK genes are now known to be located in clusters or tandem repeats of genes of the same subfamily.

DISCUSSION

The discovery that a new class of plant receptors, the LysM-RLKs, control Nod factor signaling provided a

Table I. *Expression analysis by quantitative RT-PCR of 10 LysM-RLK genes of M. truncatula*

mRNA levels were normalized against ACTIN2 and values were calculated as ratios relative to root expression levels. The averages of two independent biological experiments are presented. Root samples always have a value of 1 and SEMs are given for other samples. Bold text indicates preferential localization of gene expression. ND, Not determined.

Gene	Expression Levels Relative to Roots				Root Expression Relative to *NFP*
	Root	Nodule	Leaf	Stem	
NFP	**1**	**0.59 ± 0**	0	0.024 ± 0.02	1
LYR1	**1**	0	0	0	ND
LYR2	**1**	**1.75 ± 0.035**	0	0	0.37
LYR3	**1**	**2.90 ± 0.89**	0.23 ± 0.11	0.005 ± 0.004	6.23
LYR4	1	2.27 ± 0.59	**10.50 ± 5.78**	1.70 ± 0.95	21.56
LYR5	1	6.39 ± 0.54	**21.79 ± 0.24**	0.26 ± 0.02	2.43
LYR6	**1**	**3.80 ± 3.95**	0.26 ± 0.032	0.008 ± 0.004	12
LYK8	**1**	0.06 ± 0	0.01 ± 0.007	0	1.22
LYK9	1	0.74 ± 0.12	**2.33 ± 0.76**	0.28 ± 0.085	38.32
LYK10	**1**	**0.73 ± 0.10**	0	0	0.15

major breakthrough in our understanding of the Rhizobium symbiosis (for review, see Cullimore and Dénarié, 2003; Parniske and Downie, 2003; Riely et al., 2004; Stacey et al., 2006). Given that *M. truncatula nfp* mutants exhibit very similar phenotypes to *L. japonicus* and pea LysM-RLK mutants, it was likely that *NFP* would also encode a LysM-RLK. Our confirmation of this provides support for the genetic evidence that NFP could be a Nod factor receptor (Ben Amor et al., 2003), and we have now shown that NFP is implicated in nodule organogenesis and throughout the infection process. The evidence that NFP has three LysM domains with different potential properties for ligand recognition and a kinase domain with no apparent autophosphorylation activity provides new information on how NFP might function in Nod factor perception and transduction. Furthermore, we show that *M. truncatula* has a larger LysM-RLK gene family than Arabidopsis or rice, with other genes that may fulfill symbiotic roles.

The *NFP* Gene Controls Both Early Symbiotic Responses and Infection

NFP gene expression observed in root hairs before inoculation with *S. meliloti* is consistent with the role of NFP in controlling a rapid calcium flux, calcium spiking, and inhibition of reactive oxygen efflux within minutes of Nod factor addition to root hairs (Ben Amor et al., 2003; Shaw and Long, 2003). Moreover, this constitutive expression of *NFP* was restricted to growing and recently matured root hairs, corresponding to the susceptible zone for Nod factor responses and rhizobial infection. After rhizobial inoculation, *NFP* expression was strongly linked to nodule primordia development in the root cortex and to infection in root hairs and underlying outer cortical cells. This latter type of cell has been described in Medicago as being prepared for infection by the presence of preinfection threads (Timmers et al., 1999). In

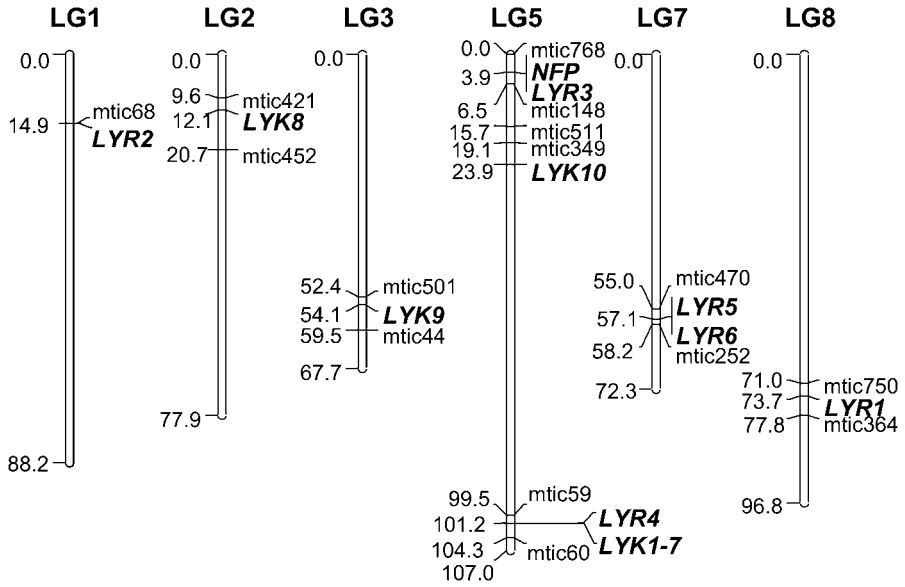

Figure 8. Genetic map positions of *M. truncatula* LysM-RLK genes. *LYK* and *LYR* genes are positioned between microsatellite markers on six of the eight *M. truncatula* linkage groups (LG). The three cases of tandemly arranged genes (*NFP*/*LYR3*, *LYK1–7*, and *LYR5*/*LYR6*) are each indicated by a single map position. *LYR4* and *LYK1–7* also have a single map position, but are not physically linked (see text). The drawing was made using MapChart (Voorips, 2002). Distances are in cM Kosambi.

mature nodules, expression coincided again with infection thread formation and with bacterial release into host cells. Using the RNAi approach, rare infections were observed and characterized by abortive infection threads with sac-like structures. Infection thread growth and morphology is therefore apparently susceptible to a reduction in NFP levels. This, together with gene expression data, indicates that NFP is implicated throughout the infection process, in particular for infection thread development, and also possibly for bacterial release.

Of the known orthologs of *NFP*, pea *SYM10* but not *L. japonicus NFR5*, is expressed in mature nodules, which might reflect the different types of nodules formed on *M. truncatula* and pea (indeterminate) compared to *L. japonicus* (determinate; Madsen et al., 2003). A major difference between these two nodule types is that only indeterminate nodules have a persistent meristem continually producing new nodule cells that can be infected by rhizobia. Therefore, this supports important roles for NFP and pea SYM10 in Nod factor signaling during the infection process in nodules. Furthermore, the absence of expression of both *NFR5* in mature *L. japonicus* nodules and *NFP* in the central tissue of mature *M. truncatula* nodules indicates that neither gene is likely to be involved in nitrogen fixation or assimilation.

NFP Might Act Upstream of Distinct Nod Factor Signaling Pathways

Functional and expression analysis of *DMI1*, *DMI2*, and *DMI3*, predicted to control Nod factor signaling downstream of *NFP*, suggests that Nod factor signaling occurs throughout infection in *M. truncatula* (Bersoult et al., 2005; Limpens et al., 2005, Hogg et al., 2006). However, the three *DMI* genes also control mycorrhization and *dmi* mutants have nonsymbiotic phenotypes (Catoira et al., 2000; Esseling et al., 2004). Because the *NFP* gene has not been shown to control anything other than Nod factor perception, our *NFP* data more directly suggest that Nod factor perception and signaling occur throughout the infection process. The occurrence of Nod factor recognition in the infection zone of *M. truncatula* nodules is corroborated by the expression pattern of *LYK3* (Limpens et al., 2005). Also, in nodules, *NFP* expression coincides with the localization of rhizobial *nod* gene transcripts and Nod factors, whereas the decline in *NFP* expression toward the nitrogen-fixing zone coincides with the decline of *nod* gene transcripts, as well as with organelle redistribution and cytoskeleton reorganization (Sharma and Signer, 1990; Schlaman et al., 1991; Timmers et al., 1998).

NFP expression is associated with two concurrent series of events described during establishment of nodulation in *M. truncatula* (Timmers et al., 1999), suggesting that *NFP* controls distinct Nod factor signaling pathways, one for symbiotic infection and one for nodule organogenesis. It is not known whether the outward wave of activation for nodule organogenesis is induced by Nod factors or Nod factor derivatives, or whether secondary signals are transmitted following epidermal Nod factor perception. The strong accumulation of fluorescent Nod factor derivatives in root hair cell walls (Goedhart et al., 2003) does not exclude the diffusion or transfer of a small proportion to inner tissues. The strong and rapid up-regulation of *NFP* expression in inner cortical cells is compatible with a long-range signal being Nod factors or Nod factor derivatives. It will be interesting to elucidate the role of a putative Nod factor receptor several cell layers distant from the site of Nod factor-producing rhizobia.

LysM-RLKs Have a Conserved LysM Triplet in Their Extracellular Regions

LysM domains are probably of prokaryotic origin and are common modules of bacterial surface proteins (Bateman and Bycroft, 2000). The combination of LysM domains with a transmembrane helice and a kinase domain is specific to the phylogenic lineage of plants and, interestingly, despite the two different gene structures found for these genes, there is never an intron within the predicted extracellular LysM coding region.

Whereas LYK3, LYK4, and *L. japonicus* NFR1 were described as having two LysM domains each (Limpens et al., 2003; Radutoiu et al., 2003), we could structurally predict three such domains each time (data not shown), as well as for the 14 other *M. truncatula* proteins studied. This indicates that three LysM domains are a general feature of plant LysM-RLKs. The Cys-X-Cys motif was always found between the three predicted LysM domains of *M. truncatula* proteins and is present in the corresponding regions of Arabidopsis and rice proteins. This suggests that disulfide bridges might participate in the spatial distribution of LysM domains and that a LysM triplet of three LysM domains separated by Cys-X-Cys motifs and linked to a kinase domain by a transmembrane helix appeared early in plant history, probably predating the division of LysM-RLKs into the two major clades, LysM-I and LysM-II.

The LysM triplet in plant LysM-RLKs might have originally consisted of the same LysM sequence repeated three times because each LysM domain has an overall 3-D fold similar to that of a bacterial LysM domain. Recent work by Mulder et al. (2006) also suggests conservation of structure between plant and bacterial LysM domains. The differences in surface charge distribution and structurally homologous amino acids between LysM1, LysM2, and LysM3 of a given protein suggest that each domain has specialized functions in terms of ligand recognition.

A LysM triplet might also be characteristic of plant nonkinase LysM proteins. During this work, we identified two *M. truncatula* genes predicted to encode such proteins with three LysM domains structurally predicted for each and showing strong homology to the glycosylphosphatidylinositol-anchored proteins

AtLYM1 (At1g21880) and AtLYM2 (At2g17120; Borner et al., 2003). Both *M. truncatula* proteins are predicted to be secreted and one to be membrane located. By analogy with the role of proteins that resemble RLK extracellular domains in RLK signaling (Jeong et al., 1999), it will be interesting to investigate whether nonkinase LysM proteins play roles in symbiotic signaling.

LysM-RLKs Have Either Classical or Nonclassical Kinase Domains

Compared to LysM domains, there is higher conservation among the kinase domains of LysM-RLKs, illustrated by the conserved predicted 3-D structures for NFP and LYK3. Despite this, we distinguished kinase domains of distinct evolutionary origin and only LysM-RLKs in clades I and III were predicted to have classically functional kinase domains. In clade II, accumulated mutations in generally conserved residues probably predated dicot/monocot divergence. For example, *M. truncatula* NFP, *M. truncatula* LYR1, and Os03g13080 have key residues not conserved and no activation loop. A similar such gene was recently identified in *Populus trichocarpa* (Stacey et al., 2006). In contrast, the *LYR5* and *LYR6* genes may be of relatively recent origin because they form a distinct phylogenetic group with no close relatives in Arabidopsis or rice. Close inspection of LYR5/6 indicates that their LysM domains are more similar to LYR than to LYK proteins, whereas their kinase domains show 59% identity to those of Arabidopsis WAK-like proteins. Molecular complexity in the LysM-RLK family has thus apparently arisen by fusion of the same LysM triplet region to different kinase domains, as for other plant RLKs (Shiu and Bleecker, 2003).

Amino acid replacements in conserved protein domains can be expected to contribute to functional diversity. Different plant LysM-RLKs may consequently have distinct modes of functioning for signal transduction, with some potentially having inactive or so-called dead kinase domains. This is supported by the absence of detectable in vitro autophosphorylation activity for the NFP kinase domain. Moreover, although we cannot exclude ligand-activated autophosphorylation, the long-lasting conservation of this type of kinase with a predicted typical 3-D structure supports an important role in signal transduction. A similar conclusion can be drawn for NFP orthologs in *L. japonicus* and pea, based on the null phenotypes of certain kinase domain mutants (Madsen et al., 2003).

Increasing evidence suggests that some dead kinase receptor kinases are signal-transducing molecules without kinase activity. Examples in animals include ErbB3 and H-Ryk, which both form heterodimers with kinase-active receptors (Kroiher et al., 2001). In plants, kinase-dead RLKs are found in three families and include AtCRR1 and AtCRR2, which have no activation loops, are nearly inactive in autophosphorylation assays, and AtCRR2 can be phosphorylated by AtACR4 (Johnson and Ingram, 2005). Whether nonclassical kinases such as NFP associate with active kinase partners or have an unusual mechanism of signal transduction is an open question.

M. truncatula Has a Larger LysM-RLK Gene Family Than the Nonlegumes Arabidopsis and Rice

Approximately 60% of the gene-rich region of the *M. truncatula* genome is sequenced and 16 expressed LysM-RLK genes have been identified. Compared to Arabidopsis and rice, with five and six LysM-RLK genes, respectively, duplication of these genes in *M. truncatula* raises many questions. Some putative orthologs can be identified across plant species, suggesting related functions, and there are some potentially *M. truncatula*-specific LYK and LYR proteins. By analogy with the role of LysM domains in recognizing *N*-acetyl-glucosamine (Steen et al., 2003, 2005) and their presence in both a chitinase of *Volvox carteri* (Amon et al., 1998) and putative Nod factor receptors, all plant LysM-RLKs may recognize β1- to β4-linked *N*-acetyl-amino sugar ligand molecules such as chitin oligomers. Furthermore, because such molecules have never been reported in plants, all plant LysM-RLKs might have roles in recognizing other organisms, for example, in the process of innate immunity.

According to Shiu et al. (2004), plant RLKs involved in development have rarely been duplicated after the dicot-monocot split, whereas those involved in defense/disease resistance have undergone many duplication events. Some *M. truncatula* LysM-RLKs are found as ESTs from elicitor/pathogen-treated tissue, but these are not highly represented in their cDNA libraries. As pointed out by Parniske and Downie (2003), the clustering of Nod factor receptor genes could facilitate recombination and hence participate in the recognition by closely related plants of different Nod factor structures. Consistent with this, *NFP* and *LYK3* are two of the 11 *M. truncatula* LysM-RLK genes known to be located in clusters or tandem repeats.

The finding that many *M. truncatula* LysM-RLK genes, like *NFP* and *LYK3*, are expressed in nodules suggests that expansion of the LysM-RLK gene family in *M. truncatula* is connected with nodulation. Seven newly identified genes (*LYR2*, *LYR3*, *LYR4*, *LYR5*, *LYR6*, *LYK9*, and *LYK10*) are expressed in nodules, and six (*LYR1*, *LYR2*, *LYR3*, *LYR6*, *LYK8*, and *LYK10*) are expressed exclusively or almost exclusively in roots and/or nodules. At least the first group of genes must fulfill roles in nodulation. The different expression patterns of the tandemly repeated genes *LYR5/6* suggest that specialization for symbiotic functions can follow gene duplication.

Large-scale genomic studies have explored why rhizobia nodulate legumes (Weidner et al., 2003; Silverstein et al., 2006). Further analysis of LysM-RLK gene families in different plant species should help elucidate which preexisting functions were adapted for Nod factor signaling. It will also be interesting to

see whether LysM-RLK expansion is a characteristic of all nodulating legumes or only of legumes like *M. truncatula*, which form indeterminate nodules. Interestingly, the *NFR1* gene of *L. japonicus* (determinate nodules) is found within a cluster of only three LysM-RLK genes compared to seven for the *M. truncatula LYK3* gene cluster (Zhu et al., 2006). Also, for the rest of the newly expanded *M. truncatula* family, only a potential ortholog of *LYR3* has so far been identified in *L. japonicus* (Zhu et al., 2006).

LysM-RLKs and Nod Factor Perception

The molecular identity of NFP supports genetic evidence that this protein is an essential part of a Nod factor receptor. In this scenario, Nod factor structure would be recognized by the extracellular LysM domains. The identification of a new *nfp* allele, *nfp-2*, mutated in the first LysM domain supports a crucial role for this domain in Nod factor recognition. Furthermore, this predicted amino acid change in LysM1 leads to strong defective phenotypes, suggesting no redundancy among the three LysM domains of NFP. Instead, only LysM1 may be needed or, consistent with the conservation of the three domains, all three may be required for optimal activity as shown for an *N*-acetylglucosaminidase of *Lactococcus lactis* (Steen et al., 2005).

In *L. japonicus*, the ortholog of NFP, NFR5, is hypothesized to dimerize with NFR1, the probable ortholog of LYK3 (Madsen et al., 2003). Until now, in *M. truncatula*, there was no evidence that NFP might associate with LYK3. However, the abnormal infection threads observed on *NFP* knockdown roots resembled those reported for *LYK3* knockdown roots (Limpens et al., 2003), suggesting that NFP and LYK3 act together at this stage of the symbiotic process. LYK4 is also implicated in infection (Limpens et al., 2003) and, interestingly, whereas LYK3 and LYK4 have practically identical extracellular LysM parts, suggesting recognition of the same ligand, their kinase domains differ, suggesting that they phosphorylate different targets. In the possible scenario of NFP-LYK3/4 heterodimers, the differences in LysM domains between NFP and LYK3/4 suggest contribution of distinct ligand recognition properties to the receptor dimer.

Different LysM-RLK complexes might be implicated at different symbiotic steps (Cullimore and Dénarié, 2003) and could possibly recognize different ligands. In animals, binding different ligands can cause heterooligomerization between different receptor combinations and stimulation of different responses. In plants, heterooligomerization of RLKs is a recurring theme and there is preliminary evidence for combinatorial heteromeric pairing in response to different ligands (Johnson and Ingram, 2005). In *M. truncatula*, the discovery of three Nod factor-binding sites, all independent of NFP, is compatible with Nod factor signaling being more complex than suggested by current models (Hogg et al., 2006).

In conclusion, it can be recalled that forward genetics screens of model legumes for mutants exhibiting no response to Nod factors identified *NFR1* and *NFR5* in *L. japonicus* and *NFP* in *M. truncatula*. Comparative genetics and RNAi led to the identification of *LYK3* and *LYK4* in *M. truncatula*. These genetic approaches thus suggested that there are at least three Nod factor receptor genes in *M. truncatula*. In this study, a genomic approach identified seven new *M. truncatula* LysM-RLK genes that are expressed in roots and nodules, suggesting a higher number of Nod factor receptor genes. This can be explained if different Nod factor receptor complexes act at different steps of the symbiotic process in such a way that mutants in Nod factor receptor genes not previously identified would not have null phenotypes, or if there is functional redundancy, suggested by the fact that no mutants other than *nfp* mutants were found with the same null phenotype (equivalent to *nfr1* mutants of *L. japonicus*; Geurts et al., 2005). The implication of new LysM-RLKs in the nodulation process in *M. truncatula* now needs to be examined using RNAi and reverse genetics resources.

MATERIALS AND METHODS

Plant Material and Growth Conditions

Medicago truncatula Jemalong A17 was used in expression and RNAi studies using growth conditions as described by Catoira et al. (2000). The *nfp-2* mutant came from ethyl methanesulfonate-mutagenized seeds (M. Harrison, unpublished data) derived from L416, a transgenic A17 line carrying the *pMtENOD11-gusA* construct (Charron et al., 2004).

Plant Transformation and Rhizobial Inoculation

Plasmid introduction into *Agrobacterium rhizogenes* ARqua1, hairy root transformation, and inoculation with *Sinorhizobium meliloti* were carried out as described by Lévy et al. (2004).

NFP Cloning

The candidate *NFP* gene was identified by the EST BE204912 and the BAC clone mth2-34m14 (Oklahoma University *M. truncatula* genome-sequencing project). For mapping, a cleaved-amplified polymorphic sequence (CAPS) was made with the primers GGTTGTTCTCGGAATCTTCG and CTGCCAAAGAAGCCAAACTT, and a PCR cycle of 94°C for 4 min, then 40 cycles of 94°C for 30 s, 50°C for 30 s, 72°C for 30 s, and, finally, 72°C for 6 min. The 456-bp products were digested with *Dde*I before loading on 2% agarose gel. For in planta complementation, a 4.6-kb *Eco*RV fragment, containing the wild-type *NFP* gene plus a 1,137-bp promoter region and a 1,665-bp 3′ region was cloned in the binary vector pCambia2201 (www.cambia.org).

Spatiotemporal Expression Analysis of the *NFP* Gene

For promoter-GUS fusions, the 1.5-kb region upstream of *NFP* was amplified (94°C for 6 min, 40 cycles at 94°C for 30 s, 55°C for 30 s, and 72°C for 1 min, and then 72°C for 5 min) with the primers GTAGGTCGAC (*Sal*I) AGAAGGGAGACGGAGAGAGG and AGCGGATCC (*BamH*I) TTGTTGTGAGGAAATGCAAA and cloned into the binary vectors pLP100 (Szabados et al., 1995) and pBI101 (Jefferson et al., 1987). Resulting plasmids were verified by sequencing. Identical expression profiles were obtained with both plasmids and results are presented for pLP100. In situ hybridization was performed as described (Limpens et al., 2005) on 14-d-old nodules with two fragments of *NFP* as probes (28–260 and 425–645).

RNAi Analysis of *NFP*

Two *NFP* inverted-repeat binary constructs were cloned into pREDROOT as described in Limpens et al. (2004). Target regions for *NFPi1* and *NFPi2* of 399 (327–725) and 532 (893–1,424) bp, respectively, were amplified using the following primer combinations: ACTAGTGGCGCGCCTTTCGCGAATATCACCTAC and GGATCCATTTAAATCTGCTTTTTCTTCCATTTG; ACTAGTGGCGCGCCTAAGCAAGCCAACAATGTAT and GGATCCATTTAAATACCCCAAAAGCGAAAACAT, where the underlined sequences were used for restriction ligation cloning. Transgenic roots were selected based on red fluorescence and subsequently inoculated with *S. meliloti* strains Sm2011 (pHC60) or GMI5622 (pHC60; a *nodFE* deletion mutant; Limpens et al., 2003, 2004). Identical results were obtained with both strains and results are presented for Sm2011 (pHC60).

Microscopic Methods

Roots were observed for bacterial infection by histochemical staining of β-galactosidase activity expressed by the plasmid pXLGD4 (Ardourel et al., 1994) for Pro_{NFP}-*GUS* analysis, and by detection of green fluorescent protein (GFP) from the plasmid pHC60 for RNAi lines (Limpens et al., 2003). GUS activity in Pro_{NFP}-*GUS* analysis of uninoculated roots was detected using X-gluc (Catoira et al., 2000). Inoculated roots and nodules were prefixed with 0.5% paraformaldehyde and nodules embedded in 4% agarose before making 100-μm-thick sections with a Bio-Rad microcut H1200 vibratome. Double detection of Pro_{NFP}-*GUS* expression and bacterial LacZ activity was carried out as described (Bersoult et al., 2005) using either X-Gal and Magenta-gluc or Magenta-Gal and X-gluc. Observations were made with an Axiophot microscope by bright field (roots) or phase contrast (nodule sections). Digital images were taken with a Leica camera and software. GFP was visualized with a Carl Zeiss LSM 510 confocal laser-scanning microscope.

Autophosphorylation Test

The sequences encoding the predicted NFP and LYK3 intracellular regions were amplified by PCR using forward primers GAATTCAAAATGAAGAGATTGAATAGAAG and GAATTCAAGAAGGAAGAAGAGAAAACT and reverse primers GTCGACTTAACGAGCTATTACAGAAGT and CTCGAGTCATCTAGTTGACAACAGATT, using the *NFP* gene and *LYK3* cDNA, respectively, as templates. PCR products were digested with *Eco*RI/*Sal*I for *NFP* or *Eco*RI/*Xho*I for *LYK3* and cloned in the pGEX-6P-1 vector (Amersham Biosciences) to produce the GST-NFP and GST-LYK3 constructs. The GST-BAK1 construct is described in Li et al. (2002). GST-LYK3, GST-NFP, and GST-BAK1 fusion proteins were expressed and purified with a method modified from Horn and Walker (1994). A 10-mL *Escherichia coli* overnight culture was transferred to 400 mL of Luria-Bertani medium and grown at 37°C to a density of about 0.8 OD_{600}. Isopropylthio-β-galactoside was added to 1 mM and cells were grown for 24 h at 16°C. The cells were collected by centrifugation, washed two times with 20 mM HEPES buffer, pH 7.5, and resuspended in 20 mL of lysis buffer (10 mM sodium phosphate buffer, pH 7.5, 500 mM NaCl, 5 mM dithiothreitol, 10 mM EDTA, and a mix of protease inhibitors [1 μg/mL of leupeptin, aprotinin, antipaine, chymostatin, and pepstatin]) and sonicated on ice for 5 min. Insoluble material was removed by centrifugation, the cleared extract was added to 800 μL of glutathione Sepharose 4B (Amersham Biotech), and incubated with gentle agitation overnight at 4°C. Beads were collected by centrifugation, washed two times with 4 mL of lysis buffer without EDTA, and covered with 800 μL of elution buffer (20 mM Tris-Cl buffer, pH 8.0, 120 mM NaCl, 20 mM glutathione, 1 μg/mL protease inhibitors). Recombinant proteins were eluted by overnight incubation at 4°C under agitation. The quality and quantity of eluted protein were checked by SDS-PAGE and Bradford assay, respectively. For kinase autophosphorylation assays, 1 μg of protein was incubated in 20 μL of kinase buffer (50 mM HEPES, pH 7.4, 10 mM $MgCl_2$, 10 mM $MnCl_2$, 1 mM dithiothreitol, 600 nM ATP, 110 nM [10 μCi] [γ-^{32}P]ATP) at 30°C for 1.5 h. The reaction was stopped by adding SDS-PAGE sample buffer and boiling for 5 min. Reactions were analyzed by SDS-PAGE and, after staining with Coomassie Brilliant Blue R250, gels were dried and analyzed by phosphor imaging.

Sequence Analysis

To search for DNA sequences of *M. truncatula* LysM domains, a database of plant peptides was first compiled, consisting of 44,509 Arabidopsis (*Arabidopsis thaliana*) proteins from Swiss-Prot TrEMBL and 28,657 *M. truncatula* peptides predicted from EST clusters in the MENS database (http://medicago.toulouse.inra.fr/MENS). The ehmmsearch program of the EMBOSS package was then used to search the database of plant peptides with the seed HMM Pfam LysM domain (accession no. PF01476). The 65 potential LysM domains thus identified were put into a fasta database, which was then used to BLAST (BLASTX with parameters −F F −G 6 −E 2 −e 0.1), nucleic acid sequence databases of *M. truncatula*, both genomic (http://www.genome.ou.edu/medicago.html) and EST clusters (http://medicago.toulouse.inra.fr/MENS). Domain structure was analyzed with Pfam (http://www.sanger.ac.uk/Software/Pfam) and SUPERFAMILY (http://supfam.mrc-lmb.cam.ac.uk/SUPERFAMILY). Signal peptides and transmembrane domains were predicted (using http://www.cbs.dtu.dk/services/SignalP and http://www.cbs.dtu.dk/services/TMHMM, respectively). Rice (*Oryza sativa*) and Arabidopsis LysM-RLKs were identified by BLAST against http://www.ncbi.nlm.nih.gov/BLAST/Genome/PlantBlast.shtml?7 using *M. truncatula* LysM domains and standard parameters. Among the candidate LysM-RLKs identified, the occurrence of the conserved Cys-X-Cys motif twice in potential extracellular domains was found to be a useful criterion for selection. Amino acid sequence alignments were made with ClustalX (Thompson et al., 1997) and minor manual adjustments were made by comparison with HCA plots to improve alignments.

Phylogeny Studies

Amino acid sequence alignment was performed using ClustalX. Distances between proteins were calculated by neighbor joining with the phylo_win program using the algorithm of the PROTDIST program of the PHYLIP package. One thousand bootstrap replicates were calculated. TreeView was used to construct trees.

EST and BAC Clones

EST clusters corresponding to newly identified genes are MtD10160 (*LYR2*), MtD20757 (*LYR3*), MtC93221 (*LYR4*), MtD13882 (*LYR5*), MtC90998 (*LYR6*), MtD06512 (*LYK8*), MtD04912 (*LYK9*), and MtD15867 (*LYK10*). BAC clones identified were mth2-34m14 (*NFP* and *LYR3*), mth2-14m21 (*LYR1*), mth4-1f18 (*LYR4*), and mth2-3c7 (*LYR5* and *LYR6*). For MtLYM1, the EST MtD01600 and the BAC clone mth2-77f21 were identified. For MtLYM2, the EST MtC30180 was identified.

Quantitative RT-PCR

Plants of wild-type *M. truncatula* Jemalong A17 were grown aeroponically as described (Catoira et al., 2000). Total RNA was extracted from leaves, stems, uninoculated roots, and 10-d-old isolated nodules using the TRIzol kit (Invitrogen), treated with DNase I, and reverse transcribed as described (El Yahyaoui et al., 2004). The quantitative RT-PCR reaction was performed in a LightCycler (Roche) on 50-fold diluted cDNA using the Master SYBR green I kit (Roche). Samples were preincubated at 95°C for 5 min, followed by 45 cycles (95°C, 5 s; 65°C, 7 s; 72°C, 15 s). Specificity of PCR amplification was checked with a heat dissociation step (from 70°C–95°C) at the end of the run. Crossing points (cycle threshold) were determined with the second derivative maximum method and the arithmetic signal baseline adjustment. Amplification efficiencies and cDNA relative abundance in each sample were determined from a standard curve established from a serial $\times 5$ dilution of cDNA. Primers (Supplemental Table I) were designed using Vector NTI (InforMax). Results were standardized to the constitutive ACTIN2 expression levels as described (Limpens et al., 2005).

Mapping New LysM-RLK Genes on the *M. truncatula* Genetic Map

CAPS or microsatellite markers were generated after nucleotide sequence comparison of a PCR-amplified region from both parents of the mapping population, Jemalong and DZA315.16 (Supplemental Table II). For CAPS markers, PCR products were digested with restriction enzymes (Supplemental Table II). Markers were analyzed on 199 F6 recombinant inbred lines derived from the mapping population and positioned between bordering microsatellite markers by MAPMAKER (T. Huguet, unpublished data; Supplemental Table III; Lander et al., 1987). PCR conditions were 94°C for 4 min,

followed by 40 cycles at 94°C for 30 s, 50°C, 55°C, or 60°C for 30 s, and 72°C for 30 s, followed by 72°C for 6 min. Marker bands were separated by electrophoresis and scored as codominant markers.

Sequence data from this article can be found in the GenBank/EMBL data libraries under accession number DQ496250.

ACKNOWLEDGMENTS

We are very grateful to Jérome Gouzy for help with in silico sequence searches and to Julie Cullimore for sequencing of *LYR4*, help with the autophosphorylation tests, and critical reading of the manuscript. We thank Françoise de Billy for advice in studying the Pro_{NFP}-*GUS* expression pattern; Jean-Jacques Bono and Charles Rosenberg for useful comments on the manuscript; Maria Harrison for provision of the mutagenized seeds from which the *nfp-2* mutant was isolated; Joseph Garcia for genetic crosses; Professor Jia Li for providing the GST-BAK1 plasmid, and Joe Clouse and Deborah Samac for cDNA clones.

Received June 4, 2006; accepted July 8, 2006; published July 14, 2006.

LITERATURE CITED

Amon P, Haas E, Sumper M (1998) The sex-inducing pheromone and wounding trigger the same set of genes in the multicellular green alga Volvox. Plant Cell **10:** 781–789

Ané JM, Kiss GB, Riely BK, Penmetsa RV, Oldroyd GE, Ayax C, Lévy J, Debellé F, Baek JM, Kalo P, et al (2004) *Medicago truncatula DMI1* required for bacterial and fungal symbioses in legumes. Science **30:** 1364–1367

Ardourel M, Demont N, Debelle F, Maillet F, de Billy F, Promé JC, Dénarié J, Truchet G (1994) *Rhizobium meliloti* lipooligosaccharide nodulation factors: different structural requirements for bacterial entry into target root hair cells and induction of plant symbiotic developmental responses. Plant Cell **6:** 1357–1374

Bateman A, Bycroft M (2000) The structure of a LysM domain from *E. coli* membrane-bound lytic murein transglycosylase D (MltD). J Mol Biol **299:** 1113–1119

Ben Amor B, Shaw SL, Oldroyd GE, Maillet F, Penmetsa RV, Cook D, Long SR, Dénarié J, Gough C (2003) The *NFP* locus of *Medicago truncatula* controls an early step of Nod factor signal transduction upstream of a rapid calcium flux and root hair deformation. Plant J **34:** 495–506

Bersoult A, Camut S, Perhald A, Kereszt A, Kiss GB, Cullimore JV (2005) Expression of the *Medicago truncatula DM12* gene suggests roles of the symbiotic nodulation receptor kinase in nodules and during early nodule development. Mol Plant Microbe Interact **18:** 869–876

Borner GH, Lilley KS, Stevens TJ, Dupree P (2003) Identification of glycosylphosphatidylinositol-anchored proteins in Arabidopsis: a proteomic and genomic analysis. Plant Physiol **132:** 568–577

Catoira R, Galera C, de Billy F, Penmetsa RV, Journet EP, Maillet F, Rosenberg C, Cook D, Gough C, Dénarié J (2000) Four genes of *Medicago truncatula* controlling components of a Nod factor transduction pathway. Plant Cell **12:** 1647–1666

Catoira R, Timmers AC, Maillet F, Galera C, Penmetsa RV, Cook D, Dénarié J, Gough C (2001) The *HCL* gene of *Medicago truncatula* controls Rhizobium-induced root hair curling. Development **128:** 1507–1518

Charron D, Pingret JL, Chabaud M, Journet EP, Barker DG (2004) Pharmacological evidence that multiple phospholipid signaling pathways link Rhizobium nodulation factor perception in *Medicago truncatula* root hairs to intracellular responses, including Ca^{2+} spiking and specific *ENOD* gene expression. Plant Physiol **136:** 3582–3593

Cullimore J, Dénarié J (2003) Plant sciences: how legumes select their sweet talking symbionts. Science **302:** 575–578

Dénarié J, Debellé F, Promé JC (1996) Rhizobium lipo-chitooligosaccharide nodulation factors: signaling molecules mediating recognition and morphogenesis. Annu Rev Biochem **6:** 503–535

El Yahyaoui F, Kuster H, Ben Amor B, Hohnjec N, Puhler A, Becker A, Gouzy J, Vernié T, Gough C, Niebel A (2004) Expression profiling in *Medicago truncatula* identifies more than 750 genes differentially expressed during nodulation, including many potential regulators of the symbiotic program. Plant Physiol **136:** 3159–3176

Endre G, Kereszt A, Kevei Z, Mihacea S, Kalo P, Kiss GB (2002) A receptor kinase gene regulating symbiotic nodule development. Nature **417:** 962–966

Esseling JJ, Lhuissier FG, Emons AM (2004) A nonsymbiotic root hair tip growth phenotype in NORK-mutated legumes: implications for nodulation factor-induced signaling and formation of a multifaceted root hair pocket for bacteria. Plant Cell **16:** 933–944

Geurts R, Fedorova E, Bisseling T (2005) Nod factor signaling genes and their function in the early stages of Rhizobium infection. Curr Opin Plant Biol **8:** 346–352

Geurts R, Heidstra R, Hadri AE, Downie JA, Franssen H, Van Kammen A, Bisseling T (1997) Sym2 of pea is involved in a nodulation factor-perception mechanism that controls the infection process in the epidermis. Plant Physiol **115:** 351–359

Goedhart J, Bono JJ, Bisseling T, Gadella TWJ (2003) Identical accumulation and immobilization of sulfated and nonsulfated Nod factors in host and nonhost root hair cell walls. Mol Plant Microbe Interact **16:** 884–892

Gualtieri G, Bisseling T (2002) Microsynteny between the *Medicago truncatula SYM2*-orthologous genomic region and another region located on the same chromosome arm. Theor Appl Genet **105:** 771–779

Hogg BV, Cullimore JV, Ranjeva R, Bono JJ (2006) The *DMI1* and *DMI2* early symbiotic genes of *Medicago truncatula* are required for a high-affinity nodulation factor-binding site associated to a particulate fraction of roots. Plant Physiol **140:** 365–373

Horn MA, Walker JC (1994) Biochemical properties of the autophosphorylation of RLK5, a receptor-like protein kinase from *Arabidopsis thaliana.* Biochim Biophys Acta **1208:** 65–74

Jefferson RA, Kavanagh TA, Bevan MW (1987) GUS fusions: β-glucuronidase as a sensitive and versatile gene fusion marker in higher plants. EMBO J **6:** 3901–3907

Jeffrey PD, Russo AA, Polyak K, Gibbs E, Hurwitz J, Massague J, Pavletich NP (1995) Mechanism of CDK activation revealed by the structure of a cyclinA-CDK2 complex. Nature **376:** 313–320

Jeong S, Trotochaud AE, Clark SE (1999) The Arabidopsis *CLAVATA2* gene encodes a receptor-like protein required for the stability of the CLAVATA1 receptor-like kinase. Plant Cell **11:** 1925–1934

Johnson KL, Ingram GC (2005) Sending the right signals: regulating receptor kinase activity. Curr Opin Plant Biol **8:** 648–656

Kalo P, Gleason C, Edwards A, Marsh J, Mitra RM, Hirsch S, Jakab J, Sims S, Long SR, Rogers J, et al (2005) Nodulation signaling in legumes requires NSP2, a member of the GRAS family of transcriptional regulators. Science **308:** 1786–1789

Kroiher M, Miller MA, Steele RE (2001) Deceiving appearances: signaling by ''dead'' and ''fractured'' receptor protein-tyrosine kinases. Bioessays **23:** 69–76

Lander ES, Green P, Abrahamson J, Barlow A, Daly MJ, Lincoln SE, Newburg L (1987) MAPMAKER: an interactive computer package for constructing primary genetic linkage maps of experimental and natural populations. Genomics **1:** 174–181

Lévy J, Bres C, Geurts R, Chalhoub B, Kulikova O, Duc G, Journet EP, Ané JM, Lauber E, Bisseling T, et al (2004) A putative Ca^{2+} and calmodulin-dependent protein kinase required for bacterial and fungal symbioses. Science **303:** 1361–1364

Li J, Wen J, Lease KA, Doke JT, Tax FE, Walker JC (2002) BAK1, an *Arabidopsis* LRR receptor-like protein kinase, interacts with BRI1 and modulates brassinosteroid signaling. Cell **110:** 213–222

Limpens E, Franken C, Smit P, Willemse J, Bisseling T, Geurts R (2003) LysM domain receptor kinases regulating rhizobial Nod factor-induced infection. Science **302:** 630–633

Limpens E, Mirabella R, Fedorova E, Franken C, Franssen H, Bisseling T, Geurts R (2005) Formation of organelle-like N_2-fixing symbiosomes in legume root nodules is controlled by *DMI2.* Proc Natl Acad Sci USA **102:** 10375–10380

Limpens E, Ramos J, Franken C, Raz V, Compaan B, Franssen H, Bisseling T, Geurts R (2004) RNA interference in *Agrobacterium rhizogenes*-transformed roots of *Arabidopsis* and *Medicago truncatula.* J Exp Bot **55:** 983–992

Madsen EB, Madsen LH, Radutoiu S, Olbryt M, Rakwalska M, Szczyglowski K, Sato S, Kaneko T, Tabata S, Sandal N, et al (2003) A receptor kinase gene of the LysM type is involved in legume perception of rhizobial signals. Nature **425:** 637–640

Mitra RM, Gleason CA, Edwards A, Hadfield J, Downie JA, Oldroyd GE, Long SR (2004a) A Ca^{2+}/calmodulin-dependent protein kinase required for symbiotic nodule development: gene identification by transcript-based cloning. Proc Natl Acad Sci USA **101:** 4701–4705

Mitra RM, Shaw SL, Long SR (2004b) Six nonnodulating plant mutants defective for Nod factor-induced transcriptional changes associated with the legume-rhizobia symbiosis. Proc Natl Acad Sci USA **101:** 10217–10222

Mulder L, Lefebvre B, Cullimore J, Imberty A (2006) LysM domains of *Medicago truncatula* NFP protein involved in Nod factor perception: glycosylation state, molecular modeling and docking of chitooligosaccharides and Nod factors. Glycobiology **16:** 801–809

Oldroyd GED, Long SR (2003) Identification and characterization of *Nodulation-Signaling Pathway 2*, a gene of *Medicago truncatula* involved in Nod factor signaling. Plant Physiol **131:** 1027–1032

Parniske M, Downie JA (2003) Plant biology: locks, keys and symbioses. Nature **425:** 569–570

Radutoiu S, Madsen LH, Madsen EB, Felle HH, Umehara Y, Gronlund M, Sato S, Nakamura Y, Tabata S, Sandal N, et al (2003) Plant recognition of symbiotic bacteria requires two LysM receptor-like kinases. Nature **425:** 585–592

Riely BK, Ané JM, Penmetsa RV, Cook DR (2004) Genetic and genomic analysis in model legumes bring Nod-factor signaling to center stage. Curr Opin Plant Biol **7:** 408–413

Schlaman HR, Horvath B, Vijgenboom E, Okker RJ, Lugtenberg BJ (1991) Suppression of nodulation gene expression in bacteroids of *Rhizobium leguminosarum biovar viciae*. J Bacteriol **173:** 4277–4287

Sharma SB, Signer ER (1990) Temporal and spatial regulation of the symbiotic genes of *Rhizobium meliloti* in planta revealed by transposon *Tn5-gusA*. Genes Dev **4:** 344–356

Shaw SL, Long SR (2003) Nod factor inhibition of reactive oxygen efflux in a host legume. Plant Physiol **132:** 2196–2204

Shiu SH, Bleecker AB (2003) Expansion of the receptor-like kinase/Pelle gene family and receptor-like proteins in Arabidopsis. Plant Physiol **132:** 530–543

Shiu SH, Karlowski WM, Pan R, Tzeng YH, Mayer KF, Li WH (2004) Comparative analysis of the receptor-like kinase family in Arabidopsis and rice. Plant Cell **16:** 1220–1234

Silverstein KAT, Graham MA, VandeBosch KA (2006) Novel paralogous gene families with potential function in legume nodules and seeds. Curr Opin Plant Biol **9:** 142–146

Smit P, Raedts J, Portyanko V, Debelle F, Gough C, Bisseling T, Geurts R (2005) NSP1 of the GRAS protein family is essential for rhizobial Nod factor-induced transcription. Science **308:** 1789–1791

Stacey G, Libault M, Brechenmacher L, Wan J, May GD (2006) Genetics and functional genomics of legume nodulation. Curr Opin Plant Biol **9:** 110–121

Steen A, Buist G, Horsburgh GJ, Venema G, Kuipers OP, Foster SJ, Kok J (2005) AcmA of *Lactococcus lactis* is an *N*-acetylglucosamininidase with an optimal number of LysM domains for proper functioning. FEBS J **272:** 2854–2868

Steen A, Buist G, Leenhouts KJ, El Khattabi M, Grijpstra F, Zomer AL, Venema G, Kuipers OP, Kok J (2003) Cell wall attachment of a widely distributed peptidoglycan binding domain is hindered by cell wall constituents. J Biol Chem **278:** 23874–23881

Szabados L, Charrier B, Kondorosi A, de Bruijn FJ, Ratet P (1995) New plant promoter and enhancer testing vectors. Mol Breed **1:** 419–423

Thompson JD, Gibson TJ, Plewniak F, Jeanmougin F, Higgins DG (1997) The CLUSTAL_X windows interface: flexible strategies for multiple sequence alignment aided by quality analysis tools. Nucleic Acids Res **15:** 4876–4882

Thoquet P, Ghérardi M, Journet EP, Kereszt A, Ané JM, Prosperi JM, Huguet T (2002) The molecular genetic linkage map of the model legume *Medicago truncatula*: an essential tool for comparative legume genomics and the isolation of agronomically important genes. BMC Plant Biol **2:** 1

Timmers AC, Auriac MC, de Billy F, Truchet G (1998) Nod factor internalization and microtubular cytoskeleton changes occur concomitantly during nodule differentiation in alfalfa. Development **125:** 339–349

Timmers AC, Auriac MC, Truchet G (1999) Refined analysis of early symbiotic steps of the Rhizobium-Medicago interaction in relationship with microtubular cytoskeleton rearrangements. Development **126:** 3617–3628

Voorips RE (2002) MapChart: software for the graphical presentation of linkage maps and QTLs. J Hered **93:** 77–78

Wais RJ, Galera C, Oldroyd G, Catoira R, Penmetsa RV, Cook D, Gough C, Dénarié J, Long SR (2000) Genetic analysis of calcium spiking responses in nodulation mutants of *Medicago truncatula*. Proc Natl Acad Sci USA **97:** 13407–13412

Walker SA, Downie JA (2000) Entry of *Rhizobium leguminosarum* bv. *viciae* into root hairs requires minimal Nod factor specificity, but subsequent infection thread growth requires *nodO* or *nodE*. Mol Plant Microbe Interact **13:** 754–762

Weidner S, Pühler A, Küster H (2003) Genomics insights into symbiotic nitrogen fixation. Curr Opin Biotech **14:** 200–205

Zhu H, Riely BK, Burns NJ, Ané JM (2006) Tracing non-legume orthologs of legume genes required for nodulation and arbuscular mycorrhizal symbioses. Genetics **172:** 2491–2499

CORRECTIONS

Vol. 142: 265–279, 2006

Arrighi J.-F., Barre A., Ben Amor B., Bersoult A., Soriano L.C., Mirabella R., de Carvalho-Niebel F., Journet E.-P., Ghérardi M., Huguet T., Geurts R., Dénarié J., Rougé P., and Gough C. The *Medicago truncatula* Lysine Motif-Receptor-Like Kinase Gene Family Includes *NFP* and New Nodule-Expressed Genes.

Plant Physiology regrets a typographical error that caused ''lysin motif'' to be incorrectly printed as ''lysine motif'' in the title, abstract, and introduction of this article.